Production and optimization of xylooligosaccharides from beech wood xylan by *Bacillus amyloliquifaciens* NRRL B-14393 xylanase and its antioxidant potential

Hadeer A. Mahmoud[a], Mona M. Rashad[a], Abeer E. Mahmoud[a], Germine M. Hamdy[b], Shadia A. Fathy[b]

[a]Department of Biochemistry, Biotechnology Research Institute, National Research Centre, Dokki 12622, Giza, Egypt, [b]Department of Biochemistry, Faculty of Science, Ain Shams University, Cairo, Egypt

Correspondence to Abeer E. Mahmoud, Department of Biochemistry, Biotechnology Research institute, National Research Centre, Dokki 12622, Giza, Egypt.
Tel: +201001294829; fax: +2033370931;
e-mail: ab_essam@yahoo.com

Received: 9 January 2022
Revised: 2 February 2022
Accepted: 10 February 2022
Published: 17 May 2022

Egyptian Pharmaceutical Journal 2022, 21:97–107

Background and objective
Xylanase is a prominent industrially applicable enzyme. The present study investigated the applicability of crude *Bacillus amyloliquifaciens* NRRL B-14393 xylanase for production of xylooligosaccharides (XOS) from beech wood xylan (BWX).
Materials and methods
Crude xylanase activity was characterized in terms of xylanolytic activities present, pH, and temperature. The effect of incubation time, enzyme dosage, and substrate concentration on XOS production was investigated by response surface methodology based on central composite design. The antioxidant potential of produced XOS was assayed by 2,2-diphenyl-1-picryl-hydrazyl-hydrate (DPPH) and H_2O_2 methods besides their correlated total phenolic content was estimated using Folin-Ciocalteu colorimetric method.
Results and conclusion
The crude enzyme extract was β-xylosidase free and proved active over a broad pH range. The enzyme was thermostable up to 70°C and maximal enzyme activity was observed at 50°C and pH 8. Functional groups and purity of BWX were identified by fourier transform infrared spectroscopy (FT-IR). XOS yield was optimized to 16.02 mg XOS/ml xylan (400.45 mg XOS/g xylan) applying 1.70 mg enzyme/g xylan, 4.91 h incubation time and 1.08%, *w/v* substrate concentration. Xylobiose and xylopentose were identified by high performance liquid chromatography (HPLC) as the hydrolysate main end products. Total phenolic content of 115 ±0.60 mg GAEq/g XOS explicated the high antioxidant capacities exhibited by produced XOS.

Keywords:
antioxidant, beech wood xylan, central composite design, optimization, xylanase, xylooligosaccharides

Egypt Pharmaceut J 21:97–107

1687-4315

Introduction

The continuous application of bio-based technologies sustains the expansion of global economy. From this perspective, it is imperative to develop biomass hydrolyzing enzymes with characteristic properties in terms of yield, efficiency, and enzyme action to regulate the overall economics of industrial level process [1,2].

Xylanases are green biocatalyst responsible for linear polysaccharide β-1,4-xylan hydrolysis into industrially significant products. The essential enzyme used for xylan hydrolysis is *endo*-1,4-β-xylanase, the enzyme cleaves the β-1,4-glycoside linkage of xylan backbone. Xylan is the second most obtainable polysaccharide in nature and accounts for about 33% of total lignocellulosic biomass. The biopolymer has a large dispersity and polymolecularity, for instance, the degree of polymerization (DP) of soft wood and hard wood xylans are 70–130 and 50–200 β-xylopyranoside units, respectively [3,4].

Xylanases are profusely existent in nature and generated by several microorganisms such as bacteria, fungi, yeast, and algae. Microbial xylanases display different substrate specificities as well as biochemical features that make this class of enzymes greatly applicable in biotechnological and industrial sectors. Overall, xylanases extensively used as an ecological molecular industrial tool in lignocellulosic biorefinery, food, feed, textile, deinking, chemical, pharmaceutical, paper, and pulp industries [5].

Nondigestible oligosaccharides retain significant physicochemical, biochemical, and physiological properties. Their role as dietary fibers and prebiotics allows their use for prebiotic formulations as well as symbiotic products industry [6]. The nondigestible sugar oligomers known as xylooligosaccharides (XOS) are an emerging prospective of xylanase. XOS are commercially produced owing to their great prebiotic potential [6], immunomodulatory activity [7], anticancerous activity [8], antimicrobial activity [9], growth regulator activity [10], and other biological activities such as antioxidant, antiallergic, anti-inflammatory, and antihyperlipidaemic activities [11,12]. Also, XOS have beneficial effect against type 2 diabetes mellitus [13] and protective effect against oxidative stress [14]. XOS play an active role in preparation of nanoparticles, hydrogels, and cosmetics [15,16].

Enzymatic hydrolysis of xylan is highly specific and the reaction operating conditions are quite mild. Meanwhile, the physicochemical approach for xylan hydrolysis may result in the formation of hazardous byproducts [17]. For the production of XOS, enzyme complex with low exo-xylanase or xylosidase activity is preferred as higher exo-xylanase activity favors xylose production [11].

Conventionally, the one factor at a time approach is extremely time consuming and requires conducting multiple expensive experiments. Therefore, optimization using multivariable techniques is favorable since they are rapid, economical, and highly efficient to optimize multivariable simultaneously. Furthermore, the interactive effects among the variables provided by multivariable method are highly advantageous [18].

Water hyacinth (*Eichhornia crassipes*) is claimed as the world's worst invasive aquatic plant due to its exceptionally rapid proliferation and congest growth, presenting severe drawbacks in navigation, irrigation, and power generation systems. Earlier we have reported the potential of the aquatic plant as cheap alternative source for microbial xylanase production through solid-state fermentation [19].

The present study targeted the optimization of XOS produced by enzymatic hydrolysis of BWX. The statistical-based approach central composite design (CCD) was used with minimal number of experimental sets. *Bacillus amyloliquifaciens* NRRL B-14393 xylanase in its crude form was used for the hydrolysis process and its biochemical characteristics required for satisfactory bioprocess were investigated. The antioxidant activity of the released XOS and their related total phenolic content were evaluated.

Materials and methods

Materials

Water hyacinth was obtained during winter season from El-Mansoureya canal, Giza, Egypt. The green parts (stems and leaves) were thoroughly washed, sliced, and then crushed to small pieces 0.5–1 cm.

Beech wood xylan, XOS standards, and *p*-nitrophenyl-β-d-xylopyranoside (*p*NPX) were of HPLC grade and obtained from Megazyme company (Bray, Ireland). Other chemicals and media were of analytical grade and purchased from Sigma-Aldrich (St. Louis, MO, USA).

Microorganism and culture conditions

Bacillus amyloliquifaciens NRRL B-14393 strain was collected from Agricultural Research Service, Peoria, IL, USA. The media composition and culture conditions were as described by Salfinger and Tortorello [20].

Enzyme production

Crude *B. amyloliquifaciens* xylanase extract was prepared by solid-state fermentation of water hyacinth under optimal conditions as described by Rashad *et al.* [19]. Briefly, 10 g of sterilized water hyacinth supplemented with 0.5%, *w/w* sucrose was inoculated with 7% of *B. amyloliquifaciens* inoculum at pH 6.0 then incubated statically for 24 h at 35°C. The crude enzyme was extracted from fermented matter as reported by Yang *et al.* [21].

Enzyme assays

Crude xylanase activity was estimated by the Nelson-Somogyi reducing sugar method [22,23]. One unit of xylanase was defined as the amount of enzyme that releases 1 μmol xylose/min under the assay conditions. β-xylosidase activity in the crude extract was measured by estimating the liberated *p*-nitrophenol from *p*NPX as described by Corrêa *et al.* [24].

Effect of pH on crude enzyme activity and stability

The activity of crude xylanase was measured in pH range of 3.0–12.0, using the appropriate buffers namely citrate (pH 3.0–4.0), acetate (pH 5–5.5), phosphate (pH 6.0–7.0), Tris-HCl (pH 8.0–10.0), and glycine-NaOH (pH 11–12) at 0.05 M. The stability of crude

xylanase at various pH values was determined by preincubating the enzyme at desired pH for 60 min at 30°C. The previously mentioned buffering systems were applied under the standard assay conditions. Enzyme activity in terms of relative activity (%) was determined under the standard assay conditions.

Effect of temperature on crude enzyme activity and stability

The maximum activity of the crude enzyme in terms of relative activity was determined at different incubation temperatures ranged from 30 to 70°C. Thermal stability of the crude xylanase was determined by incubating the enzyme at different temperatures; 30, 40, 50, 60, and 70°C for varying time intervals; 15, 30, 45, 60, 90, and 120 min. Aliquots were withdrawn at desired time intervals and cooled on ice before assaying the residual enzyme activity (%) under the standard assay conditions.

Analysis of BWX

The functional groups of BWX were identified by FT-IR using JASCO-6100 spectrometer at a spectral range of 4000–400 cm^{-1}.

Enzymatic hydrolysis of BWX xylan and XOS production

The production of XOS by enzymatic hydrolysis of BWX was achieved using crude *B. amyloliquifaciens* endoxylanase. The reaction was carried out in shaking water bath under mild shaking conditions. The effect of enzyme dosage (1.11–2.22 mg/g xylan), incubation time (1–5 h), and substrate concentration (1–3%, *w/v*) on XOS production were investigated using response surface methodology. The range of the independent variables was based on preliminary one factor optimization studies. The enzymatic reaction was carried according to optimal enzyme activity (pH 8.0 and temperature 50°C). At the end of the specified incubation time, the reaction mixture was immersed in a boiling water bath for 5 min, centrifuged at 5000 rpm for 10 min then filtered through a cellulose nitrate membrane 0.45 µm. XOS were quantified by HPLC, Shimadzu Class-VPV 5.03 (Kyoto, Japan) equipped with refractive index RID-10A Shimadzu detector and heater set at 65°C. Samples were eluted on an amino-bonded column with a mobile phase of 10 mM ammonium acetate buffer (pH 5.5)-acetonitrile with flow rate of 0.8 ml/min [25]. Xylose, xylobiose, xylotriose, xylotetraose, and xylopentaose were taken as standard references (2 mg/ml). XOS concentrations expressed as mg/ml xylan were estimated by measuring the area under respective peaks.

Experimental design

The effect of incubation time (h), enzyme dosage (mg/g xylan), and substrate concentration (%, *w/v*) on the yield of XOS (Y) were determined by three-level factors CCD with a total 20 runs. Levels were coded as −1, 0, and +1 for low, middle, and high levels, respectively. The model was face centered (α=1) with six center points. The variables were coded according to the equation:

$$x_{i=}(X_i - X_{i,0}) / \Delta X_i \ (i=1,2,3) \qquad \text{Eq. (1)}$$

where x_i is the coded value of the variable X_i, $X_{i,0}$ is the actual value of X_i at center point and ΔX_i is the step change.

The relationship between variables and response was calculated by the following quadratic regression equation [26,27]:

$$Y = \beta_o + \beta_1 X_1 + \beta_2 X_2 + \beta_3 X_3 + \beta_{11} X_1^2 + \beta_{22} X_2^2 + \beta_{33} X_3^2 + \beta_{12} X_1 X_2 + \beta_{13} X_1 X_3 + \beta_{23} X_2 X_3 \qquad \text{Eq. (2)}$$

where Y is the predicted response, β_0 is constant term, β_i (β_{1-3}) is linear coefficients, β^{ii} (β_{11-33}) is quadratic coefficients, β_{ij} (i.e., β_{12}) represents the interaction parameters; X_1, X_2, and X_3 are independent variables representing of incubation time, xylanase dosage, and substrate concentration, respectively.

The conditions of each run were summarized (Table 1). The results were statistically analyzed by Design-Expert software (version 10.0.1., Stat-Ease Inc., Minneapolis, MN, USA). Analysis of variance (ANOVA) was employed to estimate the regression model. Terms with P values less than 0.05 were considered as significant. The statistical parameters of ANOVA (SD, CV%, and R^2) were analyzed and XOS yield from BWX was optimized.

Antioxidant activity of XOS

The antioxidant activity of XOS produced under optimal reaction conditions was investigated. Different concentrations of the hydrolysate (1–6 mg/ml) were evaluated using different assays. IC_{50} designated the concentration of sample required to scavenge 50% of free radicals.

DPPH radical-scavenging assay

The antioxidant activity of XOS was measured by the scavenging effect of DPPH radicals following the method described by Veenashri and Muralikrishna [28]. The DPPH radical-scavenging activity was calculated according the following equation:

Table 1 Independent variables of the CCD model and the experimental XOS yield

Run	Coded variables			Actual variables			XOS yield (mg/ml xylan)	
	X_1	X_2	X_3	Incubation time (h)	Enzyme dosage (mg/g xylan)	Substrate concentration (%, w/v)	Observed	Predicted
1	0	0	0	3	1.665	2	15.34	14.86
2	+1	0	0	5	1.665	2	15.58	14.89
3	+1	−1	+1	5	1.11	3	4.37	4.64
4	0	0	+1	3	1.665	3	14.87	14.63
5	0	−1	0	3	1.11	2	6.76	7.33
6	−1	+1	−1	1	2.22	1	12.23	11.94
7	0	0	0	3	1.665	2	14.50	14.86
8	−1	−1	+1	1	1.11	3	7.79	7.46
9	0	0	0	3	1.665	2	15.11	14.86
10	−1	−1	−1	1	1.11	1	8.57	8.35
11	0	0	0	3	1.665	2	15.26	14.86
12	+1	−1	−1	5	1.11	1	9.148	8.86
13	+1	+1	−1	5	2.22	1	14.558	14.87
14	−1	0	0	1	1.665	2	14.442	14.83
15	+1	+1	+1	5	2.22	3	14.644	14.84
16	−1	+1	+1	1	2.22	3	14.964	15.23
17	0	0	+1	3	1.665	1	14.442	15.09
18	0	0	0	3	1.665	2	13.946	14.86
19	0	0	0	3	1.665	2	15.11	14.86
20	0	+1	0	3	2.22	2	14.702	14.22

CCD, central composite design; XOS, xylooligosaccharides.

$$\text{DPPH radical-inhibiting activity (\%)} = 1\text{-}\ (A_1/A_0) \times 100 \quad \text{Eq. (3)}$$

where A_0 is the absorbance of control and A_1 is the absorbance of sample at 517 nm.

Hydrogen peroxide (H_2O_2) scavenging assay

The potential of XOS to scavenge H_2O_2 was estimated according to typical protocol [29]. The percentage of hydrogen peroxide scavenging was calculated according the following equation:

$$\%\ \text{Scavenged}\ (H_2O_2) = ((A_0 - A_1))/(A_0) \times 100 \quad \text{Eq. (4)}$$

where A_0 is the absorbance of control and A_1 is the absorbance of sample at 230 nm.

Total phenolic acid content assay

The total phenolic content of XOS expressed as mg Gallic acid equivalent/g dry powder (mg GAE/g dry powder) was estimated using Folin-Ciocalteu colorimetric method according to the methodology described by Arruda *et al.* [30].

Statistical analysis of data

All the data were reported as the mean±SD of triplicate determinations. Results and CCD model were processed by Design-Expert software (version 10.0.1., Stat-Ease Inc., Minneapolis, MN, USA).

Results and discussion

Characterization of crude enzyme

The characterization of crude *B. amyloliquefaciens* xylanase elucidated its stability, xylanolytic activity, and suitability for XOS production from BWX.

The studied hydrolytic activity of crude xylanase extract proved the absence of β-xylosidase activity, allowing the use of enzyme in crude form for high quality XOS production. It is stipulated that β-xylosidase presence releases high amount of xylose byproduct that has inhibitory effects on endo-xylanase activity and prebiotic properties of XOS [31].

The optimal temperature, pH, acidic/alkali-stability, and thermal-stability have a striking effect on industrial application of xylanase. Optimal pH is a crucial factor for enzyme-substrate binding, substrate ionization, catalytic activity of the enzyme as well as structure of enzyme stabilization [32]. The effect of pH on crude xylanase activity and stability has been examined (Fig. 1). The crude xylanase was active over a broad pH range with a maximum activity at pH 8, whereas its pure form was reported to exhibit maximal activity at pH 9.5 by Rashad *et al.* [19]. Moreover, the crude enzyme retained more than 80% of its activity at pH range 5–7.

Figure 1

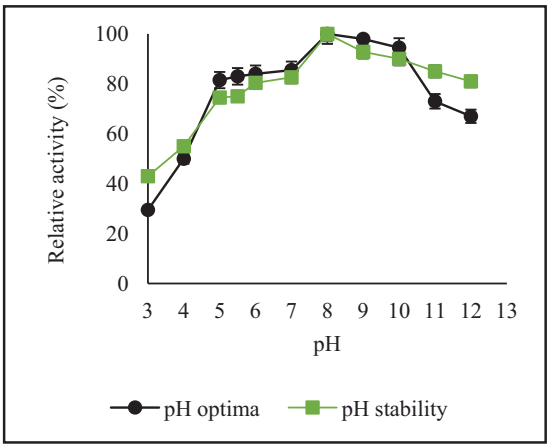

Effect of pH on xylanase activity and stability.

The crude enzyme was stable over alkaline as well as acidic pH range upon preincubation for 60 min. Alkaline tolerant xylanases have been reported from a number of bacteria, including *Bacillus* sp [33,34].

The highest xylanase activity was observed at 50°C due to the increase in the number of collisions between the reacting molecules (Fig. 2a). The decrease in enzyme activity at higher temperature might be due significant conformational changes or self-digestion of the enzyme [35]. Likewise, the observed optimal temperature of the crude xylanase was consistent with its purified form [19].

Upon studying the thermal stability of crude xylanase in the absence of xylan substrate, the results showed appreciable stability (Fig. 2b). The crude enzyme displayed an appreciable half-life up to 60°C for a period of 90 min. Furthermore, the crude enzyme was thermostable up to 70°C for 30 min and complete inhibition of the enzyme was attributed to denaturation upon longer exposure. The crude enzyme was more thermostable compared with its pure form as reported by Rashad *et al.* [19]. Suitability of xylanase complex preparations is a fundamental step when considering its use in xylan hydrolysis. The knowledge supports high XOS yield and make mass production bioprocess more feasible.

FT-IR analysis of BWX

Standard BWX was analyzed by FT-IR and the main functional groups in the sample were identified (Fig. 3). The broad band between 3400 and 3000 cm^{-1} correlated with hydroxyl groups vibrations were noted. The carbonyl stretching band was observed at 1630 cm^{-1}. The same band pattern in xylan was reported earlier [26,36]. The absorbance pattern at

Figure 2

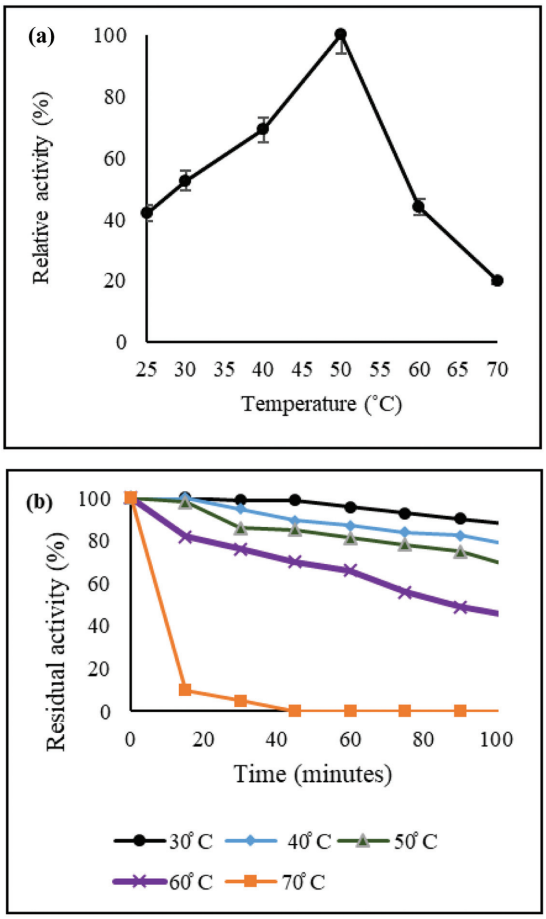

Effect of temperature on xylanase (a) activity and (b) stability.

3422, 2923, 1423, 1253, 1163, 1049, and 894 cm^{-1} are featured in xylans. Low-intensity shoulder at 1162 cm^{-1} identified the presence of arabinosyl side chains attributed to C–O–C vibration. The band at 894 cm^{-1} specified ring frequency that substantiated the presence of β-xylosidic linkage as pinpointed by Gupta *et al.* [37].

Optimization of XOS production

The effect of incubation time, xylanase dosage, and substrate concentration on XOS yield were determined by three-level factor CCD. The CCD experimental matrices consisted of a total sum of 20 sets of independent runs and a total of six central points, eight factorial points, and six axial points (Table 1). The predicted XOS yield of all the center points were 14.86±0.56 mg XOS /ml xylan, whereas the observed experimental values were varied.

The ANOVA confirmed the validity of the response model (Tables 2 and 3). The ANOVA test was used to assess the significant effect of the regression models statistically at a probability level (P) of 0.05. Otherwise, the regression models mathematically explained the

Figure 3

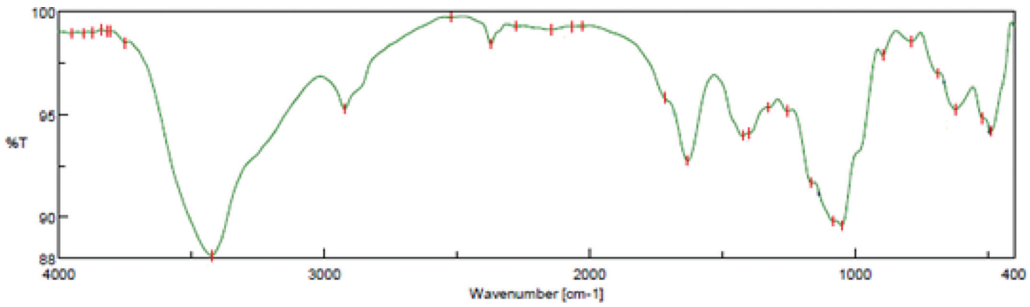

FT-IR spectrum of beech wood xylan.

relationship among the responses and the independent variables [27].

The model was significant ($P<0.0001$) with appreciable R^2 (98.33%) and adjusted R^2 (97.35%) and nonsignificant lack of fit ($P=0.4780$). The lack of fit F value of 1.09 proved insignificant relative to the pure error. Furthermore, the predicted R^2 of 0.9266 was in reasonable agreement with the adjusted R^2 of 0.9735. Adequate precision of 29.998 ratio indicated an adequate signal of the model. High coefficient of determination R^2 suggested high correlating relationship between XOS yield observed and predicted values as well as the fitness of the model. Values of % CV (4.35), SD (0.56), and predicted residual sum of squares "PRESS" (16.42) were in acceptable range validating high reliability and precision of the model. The findings were in coincidence with former study [38].

Multiple regression analysis of the model (Table 4) indicated enzyme dosage (X_2), incubation time–enzyme dosage correlation (X_1X_2), incubation time-substrate concentration correlation (X_1X_3), enzyme dosage–substrate concentration correlation (X_2X_3) and enzyme dosage^2 (X_2^2) as significant terms. Independent variables with smaller P value corresponds to higher significance of regression coefficient hence greater impact on response. Furthermore, positive and negative signs of the terms specified the effect of variables [39,40]. The estimated VIF value (1) verified the orthogonality of each term. The quadratic regression model was fitted to the following equation:

$$Y = 14.86 + 0.03\ X_1 + 3.45\ X_2 - 0.23\ X_3 + 0.61\ X_1X_2 - 0.83\ X_1X_3 + 1.05\ X_2X_3 - 4.09\ X_2^2 \quad \text{Eq. (5)}$$

where, X_1, X_2, and X_3 represent incubation time, xylanase dosage, and substrate concentration, respectively. Y is predicted XOS yield. The equation

Table 2 Statistical parameters of ANOVA

Parameter	Values	Parameter	Values
SD	0.56	R^2	0.9833
Mean	12.82	Adj. R^2	0.9735
CV%	4.35	Pred. R^2	0.9266
PRESS	16.42	Adequate precision	29.998

Adj. R^2, adjusted R^2; *ANOVA*, analysis of variance; *Pred.* R^2, predicted R^2; *PRESS*, predicted residual sum of squares.

identified the relative impact of each variable by comparative analysis of estimated coefficients.

Linear interactions of enzyme dosage ($P<0.0001$) have a strong significant impact on XOS production. The enzyme dosage–substrate concentration interaction ($P<0.0002$) and incubation time–enzyme dosage interaction ($P=0.0097$) resulted in synergetic effect on XOS yield, whereas the incubation time-substrate concentration interaction ($P<0.0012$) as well as quadric variable enzyme dosage^2 (<0.0001) has a diminishing effect on XOS yield. Previous report suggested that the linear interaction of substrate concentration and enzyme dosage has significant effect on XOS yield, whereas the interaction between substrate concentration and enzyme dosage was insignificant [41].

The graphical representations of the regression equation emphasized as 2D contour plot and 3D response surface allow identification the interaction between variables as well as the optimal predicted value of response [39,42]. The interactions between variables and their impact on XOS yield has been denoted as 2D contours and 3D response surface plots (Fig. 4a-c). Accordingly, the optimal conditions for maximum XOS yield (16.02 mg XOS/ml xylan; 400.45 mg XOS/g xylan) were xylanase dosage of 1.702 mg/g xylan, substrate concentration at 1.08%, *w/v,* and 4.91 h incubation time. Overall, the model proved fitting to design space

Table 3 Analysis of variance (ANOVA) of the model for XOS production from BWX

Source	Sum of squares	Degree of freedom	Mean square	*F* value	*P* value
CCD model	219.96	7	31.42	100.90	<0.0001
Residual	3.74	12	0.31		
Lack of fit	2.26	7	0.32	1.09	0.4780
Pure error	1.48	5	0.30		
Cor total	223.69	19			

BWX, beech wood xylan; CCD, central composite design; XOS, xylooligosaccharides.

Table 4 Estimated regression coefficients for XOS production from BWX

Factor	Coefficient estimate	Degree of freedom	*P* value	95% CI low	95% CI high	VIF
Intercept	14.86	1		14.47	15.24	
X_1	0.030	1	0.8670	–0.35	0.41	1.00
X_2	3.45	1	<0.0001	3.06	3.83	1.00
X_3	–0.23	1	0.2147	–0.62	0.15	1.00
X_1X_2	0.61	1	0.0097	0.18	1.04	1.00
X_1X_3	–0.83	1	0.0012	–1.26	–0.40	1.00
X_2X_3	1.05	1	0.0002	0.62	1.48	1.00
X_2^2	–4.09	1	<0.0001	–4.63	–3.54	1.00

BWX, beech wood xylan; CI, confidence interval; XOS, xylooligosaccharides; VIF, variation inflation factor.

and the observed values of response matched its predicted values (Fig. 5).

Degree of polymerization (DP) of produced XOS

The type of xylan from its source and the mode of action of the enzyme affect the DP of obtained XOS [43]. Released XOS in the hydrolysate were analyzed by HPLC. Chromatograms of standard sugars (xylose, xylobiose, xylotriose, xylotetraose, and xylopentaose) were depicted (Fig. 6a-e). Xylopentaose (99.52%) was the main end product followed by xylobiose (0.36%) along with very slight amount of xylose (0.12%) under conditions mimicked optimum XOS production by enzymatic hydrolysis of BWX (Fig. 7).The enzymatic production of XOS from BWX has been mentioned in several reports, but the resulted reducing sugar profile differed according to xylanolytic activities of xylanase preparations [44,45]. The slight amount of xylose in BWX hydrolysate was attributed to the purity of xylan itself because no β-xylosidase activity was detected in the crude enzyme mixture. Guido *et al.* [44] reported formation of xylose byproduct (4.97%) from BWX using β-xylosidase-free xylanase from *Thermomyces lanuginosus*.

Antioxidant potential of produced XOS

The antioxidant activity of XOS was expressed as IC_{50} by two different methods (Fig. 8). Upon interacting with DPPH, XOS were able to reduce the stable DPPH radical to the yellow-colored diphenyl-picrylhydrazine at dosage-dependent pattern indicating their scavenging abilities. Estimated IC_{50} value of XOS for DPPH scavenging was 3 mg. The percent of inhibition of XOS gradually increased and reached 61.00% at the concentration of 5 mg. The scavenging ability of XOS was attributed to either electron transfer or hydrogen transfer, thus neutralizing DPPH free radical nature [46].

Hydroxyl radical is one of oxygen radicals, which causes severe damage to cell-adjacent molecules [47]. The produced XOS was capable of scavenging H_2O_2 in a concentration-dependent manner. The IC_{50} value of XOS was 1.5 mg. It can be concluded that XOS acted as H_2O_2 scavenger by donating hydrogen atoms to reduce the H_2O_2 into H_2O.

The total phenolic content in the XOS mixture was estimated to be 115±0.60 mg GAEq/g XOS. The scavenging capacities exhibited by XOS mixture could be attributed to the transfer of hydrogen or hydroxyl molecules from the bound phenolic compounds [48]. Considering phenolic compounds molecular structure, factors such as the abundant presence of conjugated double bonds as well as the multiple hydroxyl groups provide the phenolic compounds the optimal chemical characteristics to prevent and encounter oxidative damage caused by free radicals [49].

Conclusion

The crude *B. amyloliquefaciens* free β- xylosidase xylanase broad pH stability and thermophilic

Figure 4

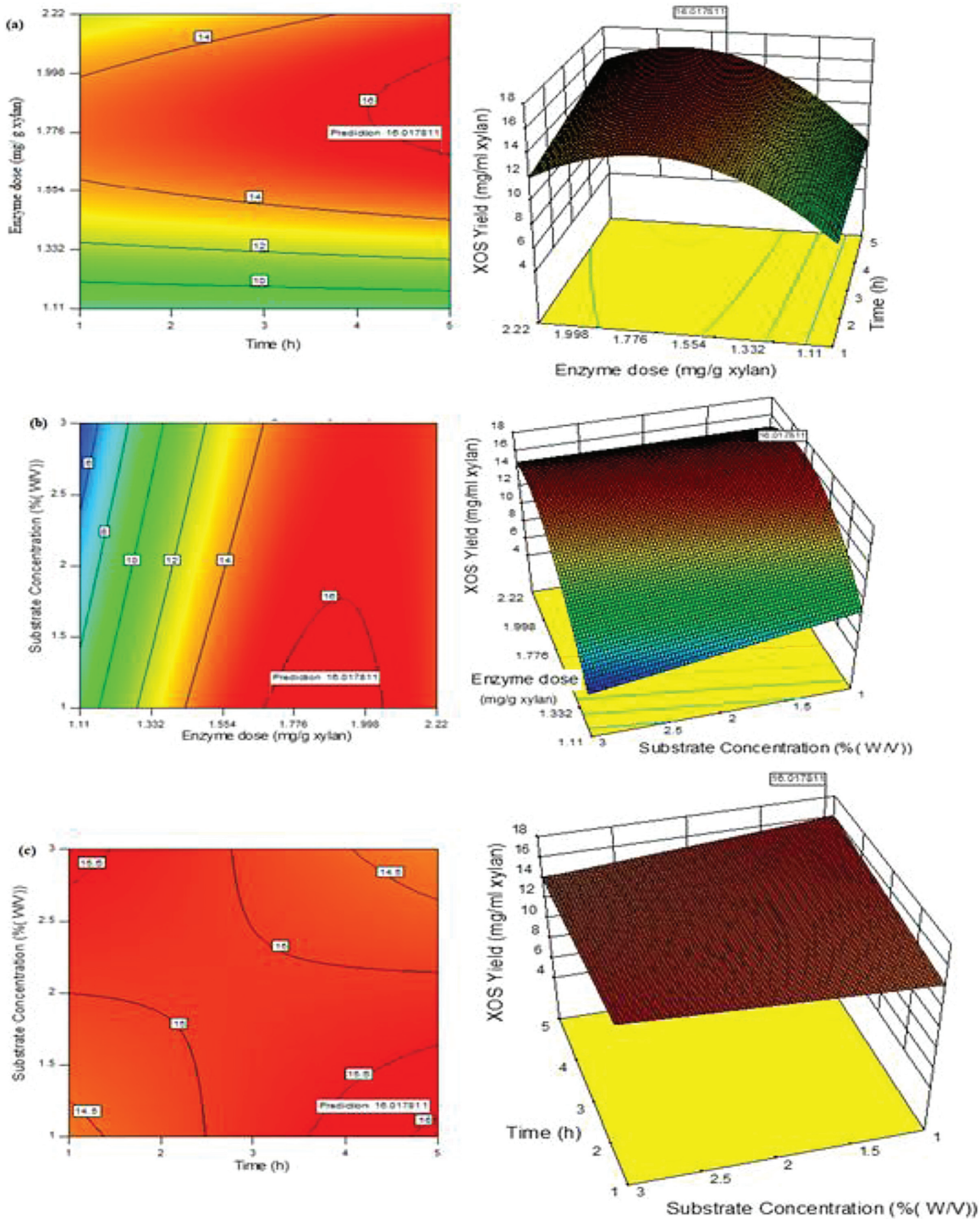

Contour and 3D response surface graphics for xylooligosaccharides yield representing the interactions between (a) time–enzyme dosage, (b) enzyme dosage–substrate concentration, and (c) time–substrate concentration.

characteristics satisfied the criteria required for efficient catalytic production of XOS from BWX. The absence of β-xylosidase activity in the crude extract enhanced the bioprocess. The FT-IR analysis of BWX indicated a typical signal pattern for xylans. The application of statistical design CCD showed that the synergistic effects of enzyme dosage–substrate concentration and incubation time–enzyme dosage interactions enabled the maximization of XOS yield (16.02 mg XOS/ml xylan; 400.45 mg XOS/g). XOS profile in the hydrolysate was determined as xylopentose and xylobiose by HPLC. The produced XOS showed acceptable antioxidant capacity and its IC_{50} values were found to be at 3 and 1.5 mg against DPPH and hydroxyl free radicals, respectively. The high antioxidant potential of produced XOS was

Figure 5

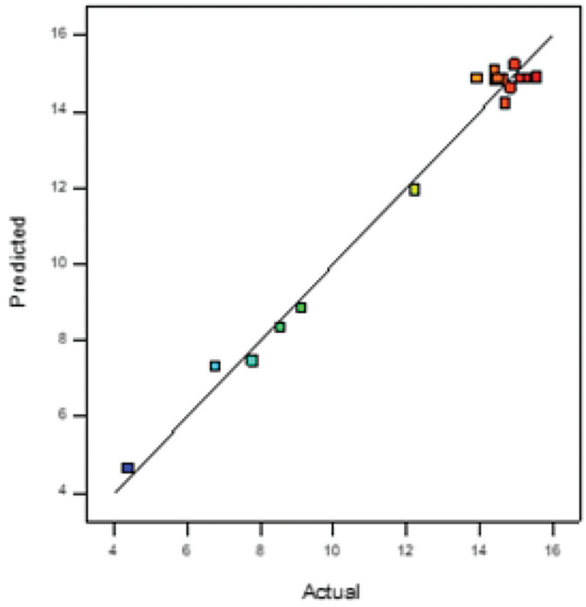

Actual observed vs. predicted xylooligosaccharides yield correlation.

Figure 6

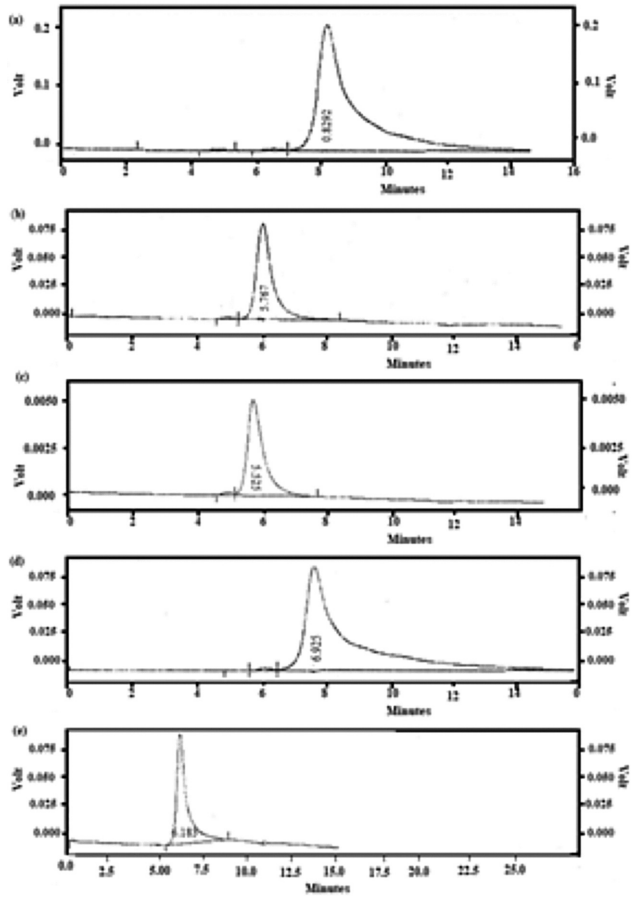

HPLC chromatograms of standard (a) xylose, (b) xylobiose, (c) xylotriose, (d) xylotetraose, and (e) xylopentaose.

Figure 7

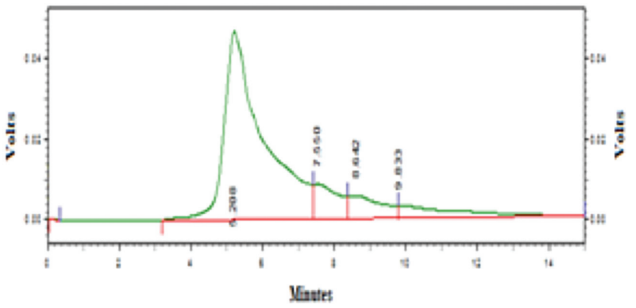

HPLC chromatogram of xylooligosaccharides produced from beech wood xylan.

Figure 8

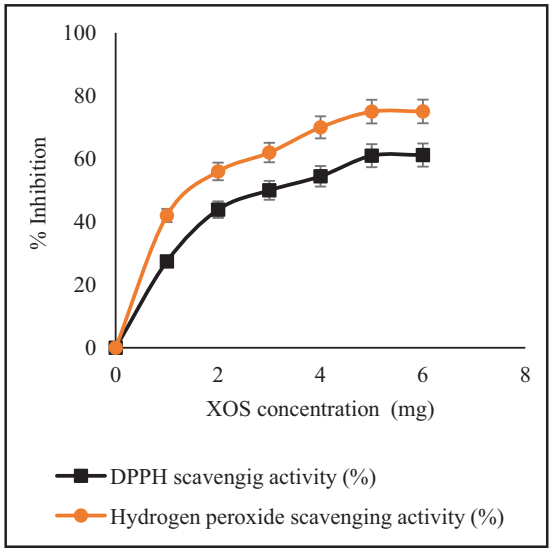

Xylooligosaccharides antioxidant activity against DPPH and hydrogen peroxide.

attributed to their estimated total phenolic content of 115±0.60 mg GAEq/g XOS. These findings suggest that this type of xylanase preparation is very promising for obtaining high XOS yield with low DP and high antioxidant capacity available for commercial production.

Financial support and sponsorship

This study was supported by the National Research Centre, Giza, Egypt (Project no. 12010606).

Conflicts of interest

There are no conflicts of interest.

References

1 Song B, Lin R, Lam CH, Wu H, Tsui T-H, Yu Y. Recent advances and challenges of inter-disciplinary biomass valorization by integrating hydrothermal and biological techniques. Renew Sust Energ Rev 2021; 135:1–19.

2 Patel AK, Dixit P, Pandey A, Singhania RR. Promising enzymes forbiomass processing. In Singh RS, Singhania R, Pandey A, Larroche C, editors. Biomass, biofuels, biochemicals. Amsterdam, NL: Elsevier; 2020. pp. 245–271.

3 Walia A, Guleria S, Mehta P, Chauhan A, Parkash J. Microbial xylanases and their industrial application in pulp and paper biobleaching: a review. 3 Biotech 2017; 7:11–22.

4 Sunna A, Antranikian G. Xylanolytic enzymes from fungi and bacteria. Crit Rev Biotechnol 1997; 17:39–67.

5 Bhardwaj N, Kumar B, Verma P. A detailed overview of xylanases: an emerging biomolecule for current and future prospective. Bioresour Bioprocess 2019; 6:1–36.

6 Vazquez M, Alonso J, Domınguez H, Parajo J. Xylooligosaccharides: manufacture and applications. Trends Food Sci Technol 2000; 11:387–393.

7 Chen HH, Chen YK, Chang HC, Lin SY. Immunomodulatory effects of xylooligosaccharides. Food Sci Technol Res 2012; 18:195–199.

8 Ghosh A, Chandra A, Dhar A, Shukla P, Baishya D. Multi-efficient thermostable endoxylanase from *Bacillus velezensis* AG20 and its production of xylooligosaccharides as efficient prebiotics with anticancer activity. Process Biochem 2021; 109:59–71.

9 Christakopoulos P, Katapodis P, Kalogeris E, Kekos D, Macris B, Stamatis H, *et al.* Antimicrobial activity of acidic xylo-oligosaccharides produced by family 10 and 11 endoxylanases. Int J Biol Macromol 2003; 31:171–175.

10 Van Doan H, Hoseinifar SH, Faggio C, Chitmanat C, Mai NT, Jaturasitha S, *et al.* Effects of corncob derived xylooligosaccharide on innate immune response, disease resistance, and growth performance in Nile tilapia (Oreochromis niloticus) fingerlings. Aquaculture 2018; 495:786–793.

11 Motta F, Andrade C, Santana M. A review of xylanase production by the fermentation of xylan: classification, characterization and applications. In Chandel AK, da Silva SS, editors. Sustainable degradation of lignocellulosic biomass-techniques, applications and commercialization. London, UK: Intech Open; 2013, pp. 251–274.

12 Shimoda K, Hamada H, Hamada H. Synthesis of xylooligosaccharides of daidzein and their anti-oxidant and anti-allergic activities. Int J Mol Sci 2011; 12:5616–5625.

13 Gobinath D, Madhu AN, Prashant G, Srinivasan K, Prapulla SG. Beneficial effect of xylo-oligosaccharides and fructo-oligosaccharides in streptozotocin-induced diabetic rats. Br J Nutr 2010; 104:40–47.

14 Wang J, Cao Y, Wang C, Sun B. Wheat bran xylooligosaccharides improve blood lipid metabolism and antioxidant status in rats fed a high-fat diet. Carbohydr Polym 2011; 86:1192–1197.

15 Martins M, Sato ACK, Ogino K, Goldbeck R. Evaluating the addition of xylooligosaccharides into alginate-gelatin hydrogels. Food Res Int 2021; 147:1–7.

16 Amorim C, Silvério SC, Prather KL, Rodrigues LR. From lignocellulosic residues to market: production and commercial potential of xylooligosaccharides. Biotechnol Adv 2019; 37:107397.

17 Gowdhaman D, Ponnusami V. Production and optimization of xylooligosaccharides from corncob by *Bacillus aerophilus* KGJ2 xylanase and its antioxidant potential. Int J Biol Macromol 2015; 79:595–600.

18 Ibrahim S, Wahab NA, Anuar AN, Bob M. Parameter optimisation of aerobic granular sludge at high temperature using response surface methodology. Int J Electr Comput Eng 2017; 7:1522–1529.

19 Rashad MM, El-Torky A, Nooman MM, Keshta AT, Mahmoud HA, Mahmoud AE. Enhanced production of cellulase-free xylanase from*Bacillus amyloliquifaciens* NNRL B-14393 by solid state fermentation of water hyacinth and its application in degradation of agricultural residues. Asian J Microbiol Biotechnol Environ Sci 2015; 17:865–877.

20 Salfinger Y, Tortorello ML, (eds.). Compendium of methods for the microbiological examination of foods. Washington, US: American Public Health Association; 2015.

21 Yang S, Yan Q, Jiang Z, Li L, Tian H, Wang Y. High-level of xylanase production by the thermophilic *Paecilomyces themophila* J18 on wheat straw in solid-state fermentation. Bioresour Technol 2006; 97:1794–1800.

22 Somogyi M. Notes on sugar determination. J Biol Chem 1952; 195:19–23.

23 Nelson N. A photometric adaptation of the Somogyi method for the determination of glucose. J Biol Chem 1944; 153:375–380.

24 Corrêa JM, Christi D, Torre CLD, Henn C, Conceição-Silva JLd, Kadowaki MK, *et al.* High levels of β-xylosidase in *Thermomyces lanuginosus*: potential use for saccharification. Braz J Microbiol 2016; 47:680–690.

25 Pu J, Zhao X, Wang Q, Wang Y, Zhou H. Development and validation of a HPLC method for determination of degree of polymerization of xylo-oligosaccharides. Food Chem 2016; 213:654–659.

26 Khat-Udomkiri N, Sivamaruthi BS, Sirilun S, Lailerd N, Peerajan S, Chaiyasut C. Optimization of alkaline pretreatment and enzymatic hydrolysis for the extraction of xylooligosaccharide from rice husk. AMB Express 2018; 8:115–124.

27 Bian J, Peng P, Peng F, Xiao X, Xu F, Sun R-C. Microwave-assisted acid hydrolysis to produce xylooligosaccharides from sugarcane bagasse hemicelluloses. Food Chem 2014; 156:7–13.

28 Veenashri B, Muralikrishna G. In vitro anti-oxidant activity of xylo-oligosaccharides derived from cereal and millet brans—a comparative study. Food Chem 2011; 126:1475–1481.

29 Ruch RJ, Cheng S-j, Klaunig JE. Prevention of cytotoxicity and inhibition of intercellular communication by antioxidant catechins isolated from Chinese green tea. Carcinogenesis 1989; 10:1003–1008.

30 Arruda HS, Pereira GA, Pastore GM. Optimization of extraction parameters of total phenolics from *Annona crassiflora* Mart. (Araticum) fruits using response surface methodology. Food Anal Methods 2017; 10:1–10.

31 Reddy SS, Krishnan C. Production of high-pure xylooligosaccharides from sugarcane bagasse using crude β-xylosidase-free xylanase of *Bacillus subtilis* KCX006 and their bifidogenic function. LWT-Food Sci Technol 2016; 65:237–245.

32 Sohpal VK, Dey A, Singh A, (eds.). Investigate of process parameters on xylanase enzyme activity in Melanocarpus albomyces batch culture. London, U. K: Proceedings of the World Congress on Engineering 2010. 1–5

33 Yadav P, Maharjan J, Korpole S, Prasad GS, Sahni G, Bhattarai T, *et al.* Production, purification, and characterization of thermostable alkaline xylanase from *Anoxybacillus kamchatkensis* NASTPD13. Front Bioeng Biotechnol 2018; 6:65.

34 Khusro A, Kaliyan BK, Al-Dhabi NA, Arasu MV, Agastian P. Statistical optimization of thermo-alkali stable xylanase production from *Bacillus tequilensis* strain ARMATI. Electron J Biotechnol 2016; 22:16–25.

35 Fu D, Li C, Lu J, Rahman Au, Tan T. Relationship between thermal inactivation and conformational change of *Yarrowia lipolytica* lipase and the effect of additives on enzyme stability. J Mol Catal B Enzym 2010; 66:136–141.

36 Ruzene DS, Silva DP, Vicente AA, Gonçalves AR, Teixeira JA. An alternative application to the Portuguese agro-industrial residue: wheat straw. Appl Biochem Biotechnol 2008; 147:85–96.

37 Gupta S, Madan R, Bansal M. Chemical composition of Pinus caribaea hemicellulose. Tappi J 1987; 70:88–90.

38 Xiao X, Wang C-Z., Bian J, Sun R-C. Optimization of bamboo autohydrolysis for the production of xylo-oligosaccharides using response surface methodology. RSC Adv 2015; 5:106219–106226.

39 Chollom MN, Rathilal S, Swalaha FM, Bakare BF, Tetteh EK. Comparison of response surface methods for the optimization of an upflow anaerobic sludge blanket for the treatment of slaughterhouse wastewater. Environ Eng Res 2020; 25:114–122.

40 Baş D, Boyacı IH. Modeling and optimization I: usability of response surface methodology. J Food Eng 2007; 78:836–845.

41 Singh RD, Nadar CG, Muir J, Arora A. Green and clean process to obtain low degree of polymerisation xylooligosaccharides from almond shell. J Clean Prod 2019; 241:118237–118245.

42 Qiao D, Hu B, Gan D, Sun Y, Ye H, Zeng X. Extraction optimized by using response surface methodology, purification and preliminary characterization of polysaccharides from *Hyriopsis cumingii*. Carbohydr Polym 2009; 76:422–429.

43 Peng F, Ren J-L., Xu F, Bian J, Peng P, Sun R-C. Comparative study of hemicelluloses obtained by graded ethanol precipitation from sugarcane bagasse. J Agric Food Chem 2009; 57:6305–6317.

44 Guido E, Silveira J, Kalil S. Enzymatic production of xylooligosaccharides from beechwood xylan: effect of xylanase preparation on carbohydrate profile of the hydrolysates. Int Food Res J 2019; 26:713–721.

45 Rajagopalan G, Shanmugavelu K, Yang K-L. Production of prebiotic-xylooligosaccharides from alkali pretreated mahogany and mango wood sawdust by using purified xylanase of *Clostridium strain* BOH3. Carbohydr Polym 2017; 167:158–166.

46 Oyaizu M. Studies on products of browning reaction antioxidative activities of products of browning reaction prepared from glucosamine. Jpn J Nutr Diet 1986; 44:307–315.

47 Ebrahimzadeh MA, Nabavi SM, Nabavi SF, Bahramian F, Bekhradnia AR. Antioxidant and free radical scavenging activity of *H. officinalis L. var. angustifolius*, *V. odorata*, *B. hyrcana* and *C. speciosum*. Pak J Pharm Sci 2010; 23:29–34.

48 Feng S, Luo Z, Zhang Y, Zhong Z, Lu B. Phytochemical contents and antioxidant capacities of different parts of two sugarcane (Saccharum officinarum L.) cultivars. Food Chem. 2014; 151:452–458.

49 Bendary E, Francis R, Ali H, Sarwat M, El Hady S. Antioxidant and structure–activity relationships (SARs) of some phenolic and anilines compounds. Ann Agric Sci 2013; 58:173-181.